Ionics (2018) 24:3591–3599
https://doi.org/10.1007/s11581-018-2474-x

ORIGINAL PAPERS

Cobalt disulfide nanosphere dispersed on multi-walled carbon nanotubes: an efficient and stable electrocatalyst for hydrogen evolution reaction

Huanhuan Liu[1] · Ping He[1,2] · Lingpu Jia[1] · Mingqian He[3] · Xingquan Zhang[4] · Shuai Wang[1] · Xiaojuan Zhang[1] · Caixia Li[1] · Ying Zhang[1] · Faqin Dong[5]

Received: 24 December 2017 / Revised: 25 January 2018 / Accepted: 26 January 2018 / Published online: 16 February 2018

Abstract

Novel cobalt disulfide on multi-walled carbon nanotubes (CoS_2/MWCNTs) was synthesized via a facile one-step hydrothermal method in the presence of cetyltrimethyl ammonium bromide. The physical properties of as-prepared materials were characterized by Fourier transform infrared spectrum, X-ray diffraction, Raman spectrum, and scanning electron microscopy techniques. Physical characterizations revealed that cattierite CoS_2 nanospheres dispersed on the surface of MWCNTs uniformly. In addition, electrochemical performances of as-prepared materials for hydrogen evolution reaction were investigated by polarization curves, Tafel plots, and electrochemical impedance spectrum in 0.50 M H_2SO_4 electrolyte. It was demonstrated that MWCNT-based electrode exhibited almost no current response while CoS_2/MWCNT nanocomposite-based electrode exhibited better electrochemical performances than pure CoS_2-based electrode, including lower potential of − 257 mV for 10 mA cm^{-2} and smaller Tafel slope of 83 mV dec^{-1}. Furthermore, CoS_2/MWCNT nanocomposite retained its high activity even after 1000 cycles of cyclic voltammetry scans, demonstrating superior stability under acidic condition. The enhanced electrocatalytic activity of CoS_2/MWCNT nanocomposite-based electrode was ascribed to more exposed sulfur edges of CoS_2, larger accessible surface area, and higher conductivity derived from MWCNTs. The results suggested that CoS_2/MWCNT nanocomposite had a potential application to hydrogen evolution reaction.

Keywords Cobalt disulfide · Multi-walled carbon nanotubes · Electrocatalyst · Hydrogen evolution reaction

Introduction

In recent years, renewable energy has become an urgent issue on consideration of alleviating global warming and lessening our reliance on fossil fuels [1, 2]. Exploitation of abundant and renewable energy sources has attracted much attention [3, 4]. Unlike fossil fuels, hydrogen is considered as a clean carrier for energy storing and transporting [5, 6]. It is regarded as the most promising candidate for replacing fossil fuels in energy devices because of its numerous advantages, such as satisfactory recyclability, free pollution, and high efficiency when consumed [7–9]. However, hydrogen does not exist abundantly on earth, and we have to prepare it before use. Therefore, it is of great practical significance to develop highly efficient hydrogen production technology.

Among a great deal of techniques for hydrogen generation (steam methane reforming, coal gasification, chlor-alkali electrolyzers and water-alkali electrolyzers, etc.),

✉ Ping He
49416151@qq.com

1 School of Materials Science and Engineering, Southwest University of Science and Technology, Mianyang 621010, People's Republic of China

2 Mianyang Kingtiger New Energy Technology Co. Ltd., Mianyang 621000, People's Republic of China

3 Sichuan Changhong New Energy Technology Co. Ltd., Mianyang 621000, People's Republic of China

4 Center of Analysis and Test, Southwest University of Science and Technology, Mianyang 621010, People's Republic of China

5 Key Laboratory of Solid Waste Treatment and Resource Recycle of Ministry of Education, Southwest University of Science and Technology, Mianyang 621010, People's Republic of China

electrocatalytic water splitting offers an attractive avenue to convert electricity harvested from water into high-purity hydrogen without any pollution and emission of carbon dioxide; therefore, it has been regarded as a clean energy technology enabling a hydrogen economy in the future [10–12]. Water splitting consists of two half reactions: the oxygen evolution reaction (OER) and the hydrogen evolution reaction (HER) [13–15]. The slow kinetics and transfer of multiple electrons in water splitting can result in a considerable electrochemical overpotential, which is energy consumptive. Hence, it is desirable to develop highly efficient electrocatalysts with low overpotential toward water electrolysis to accelerate the HER rate and to thus improve the energy conversion efficiency.

Nowadays, platinum-based catalysts are considered to be the state-of-the-art electrocatalysts for HER owing to their low overpotential and high electroactivity in acidic media [16, 17]. However, the extreme scarcity, high cost, and limited durability severely restrict their widespread utilization in hydrogen production through water splitting on a global scale [18–20]. Therefore, researchers have been exploring earth abundant, stable, and efficient hydrogen evolution electrocatalysts with great enthusiasm to alternate commercially available Pt-based electrocatalysts in the past few years, and transition metals (Fe, Co, and Ni) and their compounds (carbides, nitrides, and phosphides) are considered as promising substitutes for platinum-based electrocatalysts [21–24]. Among these materials, transition metal chalcogenides account for the largest proportion [25, 26].

Compared with other transition metal sulfides, cobalt disulfides (CoS_2) are more attractive in energy storage and conversion for the facile preparation method and favorable thermal stability [27–29]. It was reported that CoS_2 exhibited better overall performances than FeS_2 and NiS_2 in HER due to its intrinsically metallic features and disulfide-terminated edges as active sites [30]. Despite the advantages above, the electronic conductivity and acidic durability of CoS_2 still need to be enhanced in consideration of electrocatalytic performances and energy consumption.

In principle, the electrocatalytic performances of electrocatalysts can be enhanced through the following two approaches. One is to tailor the size of electrocatalyst particles into nanoscale to increase the specific surface area [31]. The other is to incorporate electrocatalysts with large-surface substrates, such as carbon materials, to modulate the electronic structure on the surface of electrocatalysts, which is beneficial to enhance the conductivity [32, 33].

As one kind of carbon materials, carbon nanotubes (CNTs) attract researchers' attention for the applications in electrochemical energy storage and transformation devices due to the structural integrity, large surface area, compact arrangement, and favorable mesoporosity [34, 35]. CNTs are mainly divided into two categories: single-walled carbon nanotubes (SWCNTs) and multi-walled carbon nanotubes (MWCNTs). MWCNTs have advantages of large specific surface area, good conductivity, and structural flexibility, and thus, MWCNTs are used to improve the electronic conductivity and stability of HER electrocatalysts in the long-term operation [36, 37]. Based on the considerations above, CoS_2/MWCNT nanocomposite is likely to be an efficient and stable electrocatalyst for HER.

Herein, CoS_2/MWCNT nanocomposite was successfully synthesized through a one-step hydrothermal method with conductive matrix of acid-treated MWCNTs and assistant of cetyltrimethyl ammonium bromide (CTAB), working as surfactant and soft template. The introduction of MWCNTs alleviated the aggregation of as-prepared CoS_2, and furthermore, it enhanced the conductivity and electrocatalytic activity of CoS_2. The results showed that CoS_2/MWCNT nanocomposite exhibited excellent electrocatalytic activity and favorable stability for HER in acidic medium.

Materials and methods

Reagents and materials

$CoCl_2 \cdot 6H_2O$, CTAB, HNO_3, and C_2H_5OH (> 99.95 wt.%) were analytical grade and purchased from Chengdu Kelong Chemical Reagent Factory (Chengdu, China). CH_4N_2S and H_2SO_4 were analytical grade and purchased from Aldrich Chemical Reagent Co., Ltd., (Shanghai, China). Nafion solution (5 wt.%) was supplied by Jinan Henghua Chemical Reagent Factory (Jinan, China). The doubly distilled water used throughout the whole experiment was obtained from a Millipore system.

Commercial MWCNTs (outer diameter × inner diameter × length 20~40 nm × 10~15 nm × 5~15 μm, purity > 95%), purchased from Chengdu Institute of Organic Chemistry, Chinese Academy of Science (Chengdu, China), were treated with the mixed solution of concentrated H_2SO_4 and HNO_3 (volume ratio of 3:1) for 2 h with ultrasonication to remove the impurities and endow the surface with hydrophilic carboxylic acid groups. After the reaction, the obtained sample was filtered off, washed with distilled water, and dried at 80 °C under vacuum for 24 h.

Preparation of CoS_2/MWCNT nanocomposite

Shown in Scheme 1 was schematic illustration of the preparation of CoS_2/MWCNT nanocomposite based on hydrothermal method. In a typical synthesis, 0.15 g acid-treated MWCNTs was firstly added into 50 mL deionized water, and then, the mixture was stirred ultrasonically for 1 h at room temperature, resulting in a homogeneous suspension. Subsequently, 0.36 g CTAB as surfactant along with soft

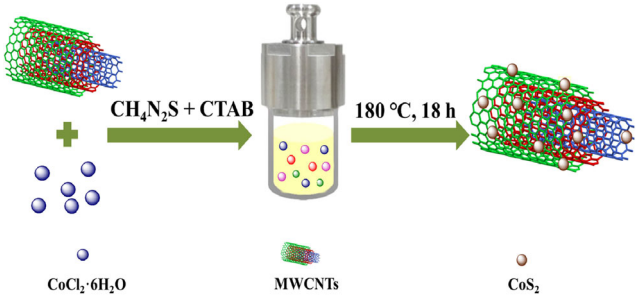

Scheme 1 Schematic illustration of synthetic procedure of CoS_2/MWCNT nanocomposite

template and 1.04 g $CoCl_2 \cdot 6H_2O$ as cobalt source were added into the above suspension, followed by mechanical stirring for 30 min. Afterwards, 1.55 g thiourea was added as sulfur precursor and reductant. Then, pH was adjusted to 6.5 by dropping 0.10 M HCl solution, and the suspension was diluted to 80 mL, followed by ultrasonication for 1 h. The final suspension was transferred into a 100 mL Teflon-lined autoclave and then heated at 180 °C for 18 h. As the autoclave cooled, the precipitate was collected, washed with distilled water and absolute ethanol thoroughly, and further dried at 60 °C for 24 h in air. The obtained substance was denoted as CoS_2/MWCNT nanocomposite.

For comparison, pure CoS_2 was synthesized according to the similar procedure above without addition of MWCNTs.

Preparation of modified electrodes

Prior to modification, glassy carbon electrode (GCE, Φ = 3 mm) was polished with 500 and 50 nm aluminum oxide powders to a mirror-like appearance, respectively, and then washed successively with ethanol and doubly distilled water for several times. Subsequently, the cleaned GCE was gently blown under a nitrogen stream.

The fabrication procedure of working electrodes was as follows. Five milligram as-prepared CoS_2/MWCNT nanocomposite and 30 μL 5 wt.% of Nafion solution were dispersed in 1.0 mL solution composed of water and ethanol with a volume ratio of 1:1, followed by ultrasonication for 30 min. Subsequently, 5.0 μL as-prepared dispersion was dropped onto the surface of a polished GCE and naturally dried in air at room temperature to form uniform films. And the CoS_2/MWCNT nanocomposite-modified GCE (CoS_2/MWCNTs/GCE) with a mass loading of 0.35 mg cm^{-2} was obtained.

For comparison, MWCNT-modified GCE (MWCNTs/GCE) and CoS_2-modified GCE (CoS_2/GCE) were fabricated according to the similar process above.

Characterization of as-prepared materials

The morphologies of as-prepared materials were investigated with scanning electron microscope (SEM) images acquired from Ultra 55 microscope (Carl Zeiss AG, Germany). The crystalline structures of as-prepared materials were characterized by X-ray diffraction (XRD) (X' Pert PRO, Netherlands) with Cu K_α radiation (λ = 0.154060 nm) and recorded in 2θ range from 10° to 80° at a speed of 2° min^{-1}. Fourier transform infrared spectra (FTIR) of as-prepared materials were obtained with a Fourier transform infrared spectrometer (Nicolet 5700, USA) in the wavenumber range of 4000~1000 cm^{-1} with KBr pellet. Raman spectra of as-prepared materials were characterized by InVia (Renishaw Instrument Co., UK) in the wavenumber range of 2500~100 cm^{-1}.

Electrochemical measurements

All electrochemical measurements were conducted in 0.50 M H_2SO_4 solution with a three-electrode test system comprising the platinum electrode as counter electrode and as-prepared material-modified GCE as working electrode referred to saturated calomel electrode (SCE). The electrolyte was purged with high-purity nitrogen (99.999%) before electrochemical measurements. Electrochemical impedance spectroscopy (EIS) measurement was carried out with a PARSTAT 2273 electrochemical workstation (Princeton Applied Research, USA). Tafel plot, polarization curves, and cyclic voltammetry (CV) curves were obtained with a CHI 760C electrochemical workstation (CH Instruments, China). All the reported potentials were calibrated to the reversible hydrogen electrode (RHE) scale at 298 K on the basis of Nernst equation as follows:

$$E_{RHE} = E_{SCE} + 0.059\ pH + 0.242\ V \quad (1)$$

Results and discussion

Physical characterizations of as-prepared materials

FTIR spectra analysis

Shown in Fig. 1 were FTIR spectra of raw MWCNTs and acid-treated MWCNTs. The weak bands located at 2915 and 2835 cm^{-1} in curve a corresponded to -CH stretching vibration. The bands at 1384 and 1113 cm^{-1} were ascribed to stretching vibration of C-C and C-O, respectively. The strong bands observed at 3435 cm^{-1} and the weak one at 1632 cm^{-1} were attributed to the stretching vibration and bending vibration, respectively, arisen from trace amounts of water [38, 39]. Compared with curve a, FTIR spectrum of acid-treated MWCNTs (curve b) exhibited an additional band at 1710 cm^{-1}, corresponding to stretching vibration of C=O of -COOH group [40]. This additional band indicated

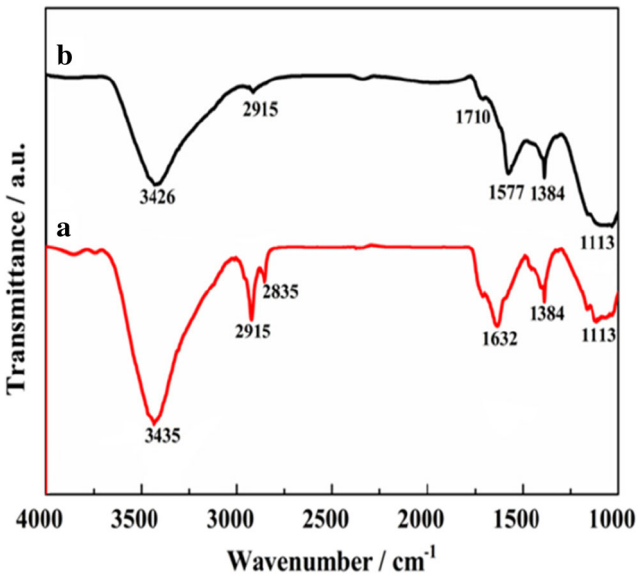

Fig. 1 FTIR spectra of raw MWCNTs (**a**) and acid-treated MWCNTs (**b**)

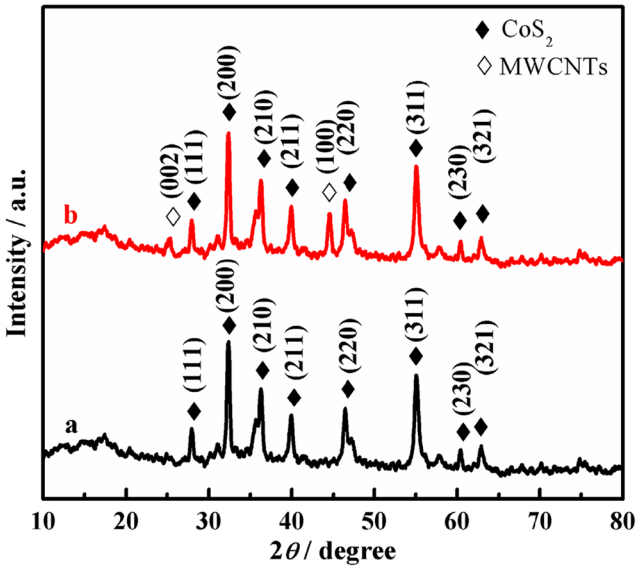

Fig. 2 XRD patterns of CoS_2 (**a**) and CoS_2/MWCNTs (**b**)

hydrophilic -COOH group on the wall and port of MWCNTs, which further enhanced the dispersity of MWCNTs.

XRD analysis

For confirming the as-prepared CoS_2 and CoS_2/MWCNTs, XRD patterns are shown in Fig. 2. As for pure CoS_2 (curve a), the diffraction peaks at 27.9°, 32.4°, 36.3°, 40°, 46.4°, 55.1°, 60.4°, and 63.04° corresponded to the lattice planes (111), (200), (210), (211), (220), (311), (230), and (321) of cattierite CoS_2 (JCPDS No. 41-1471), respectively [41]. Compared with pure CoS_2, the diffraction angle and intensity of CoS_2/MWCNTs (curve b) did not change obviously except that two additional peaks appeared at 26.1° and 44.5°, which corresponded to the lattice planes (002) and (100) of hexagonal graphite-like structure of MWCNTs, respectively, implying the successful combination of CoS_2 and MWCNTs [42].

Raman spectra analysis

Raman spectra in Fig. 3 showed the structural information of MWCNTs and CoS_2/MWCNTs. As seen from the Raman spectrum of MWCNTs (curve a), there were characteristic D band and G band at 1360 and 1589 cm^{-1}, respectively. The D band arose from sp^3 hybridization of carbon and the G band was associated with sp^2-bonded graphite-like carbon atoms. Shown in curve b, the peaks at 190, 471, and 672 cm^{-1} signified the successful fabrication of CoS_2, which was consistent with the results of XRD analysis [41]. The co-existence of peaks at 1360 and 1589 cm^{-1} of MWCNTs and peaks at 190, 471, and 672 cm^{-1} of CoS_2 verified the fabrication of CoS_2/MWCNT composite, which was in well agreement with the results obtained from XRD analysis. Furthermore, it was obvious that the ratio of I_D/I_G of CoS_2/MWCNTs was larger than that of pure MWCNTs, indicating that the structure of MWCNTs was destroyed during the hydrothermal process, and thus, more defect sites were exposed [43].

SEM analysis

Shown in Fig. 4 were SEM images of CoS_2, MWCNTs, and CoS_2/MWCNTs. As can be seen from Fig. 4a, CoS_2 was sphere-like particles with a diameter of 0.7 μm and it stacked loosely, which indicated that CoS_2 particles aggregated together during hydrothermal process. It was worth noting that MWCNTs constructed a conductive network, providing a great deal of attachment sites for CoS_2. During the

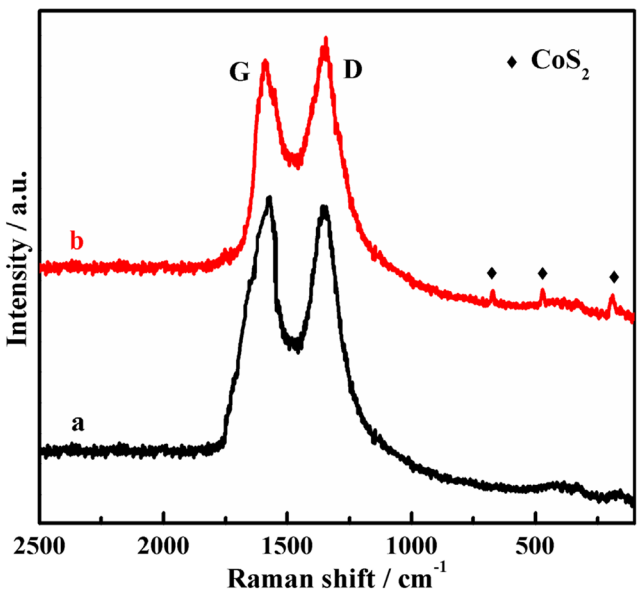

Fig. 3 Raman spectra of MWCNTs (**a**) and CoS_2/MWCNTs (**b**)

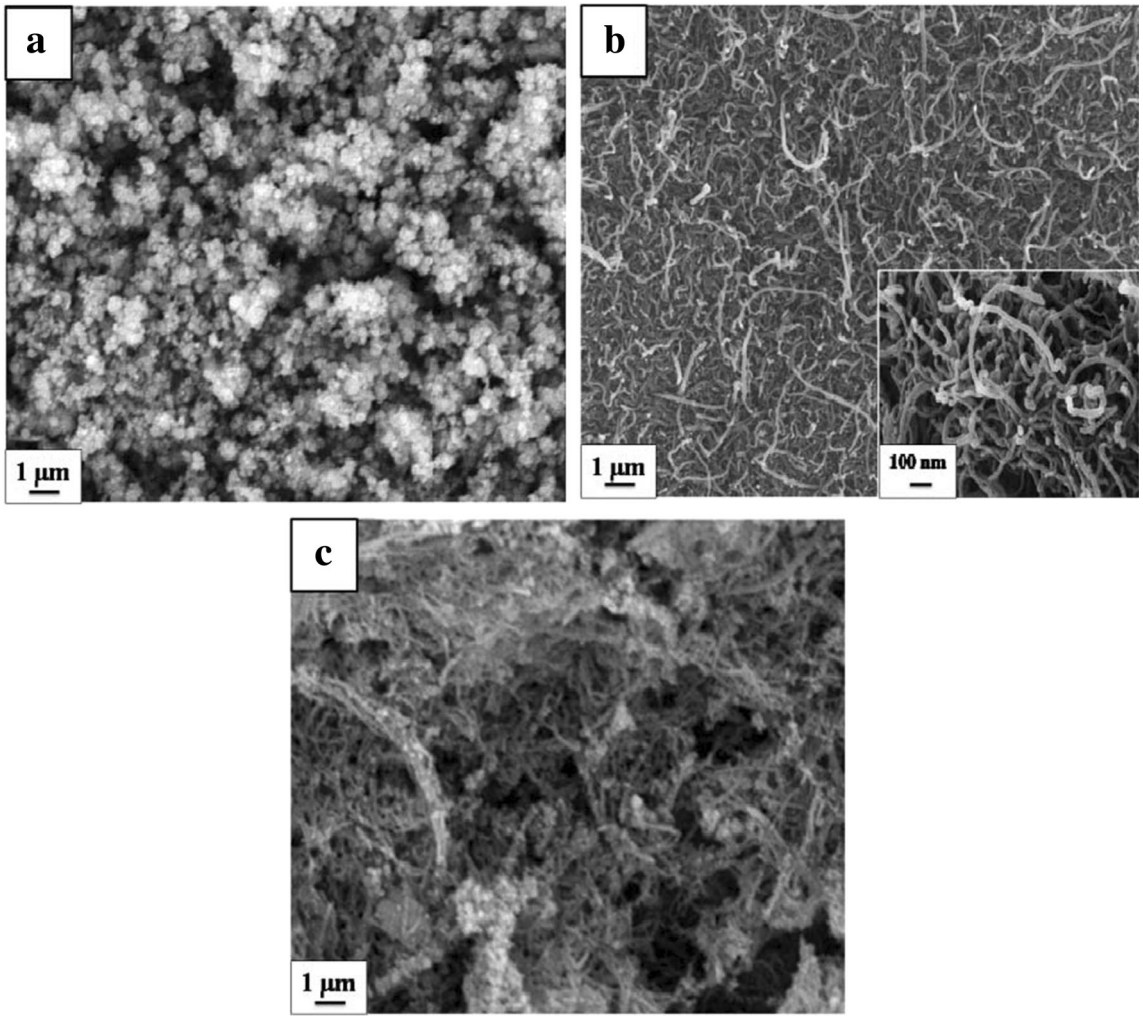

Fig. 4 SEM images of CoS_2 (**a**), MWCNTs (**b**), and CoS_2/MWCNTs (**c**)

hydrothermal process, CoS_2 adhered onto the surface of MWCNTs and combined well with MWCNTs (Fig. 4c). Notably, the aggregation of CoS_2 was relived, and the diameter of CoS_2 decreased with the introduction of MWCNTs, leading to a much larger specific surface area and thus more exposed electroactive sites.

Electrochemical performances of as-prepared modified electrodes

In order to investigate the influence of MWCNTs on the electrocatalytic performances of CoS_2 for HER, polarization curves of MWCNTs/GCE, CoS_2/GCE, and CoS_2/MWCNTs/GCE were tested in 0.50 M H_2SO_4 solution. As shown in Fig. 5, it was clearly observed that the potential of CoS_2/MWCNTs/GCE was more positive than that of CoS_2/GCE at the same current density. The potentials of CoS_2/GCE and CoS_2/MWCNTs/GCE at the current density of 10 mA cm^{-2} were − 290 and −257 mV, respectively, demonstrating higher electrocatalytic activity of CoS_2/MWCNTs/GCE. When

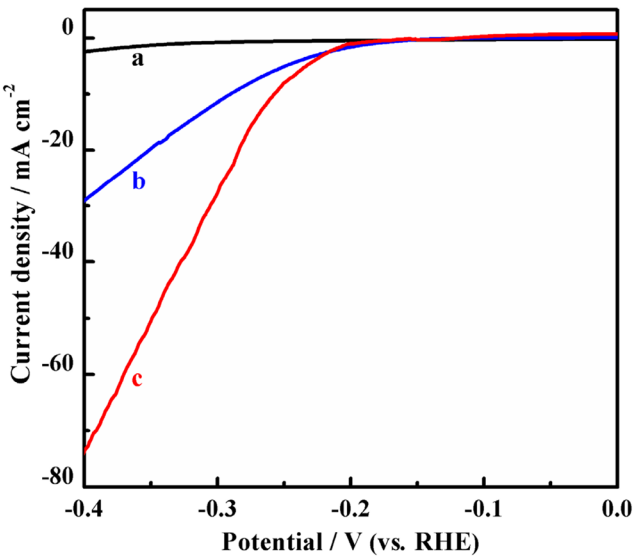

Fig. 5 Polarization curves of MWCNTs/GCE (**a**), CoS_2/GCE (**b**), and CoS_2/MWCNTs/GCE (**c**) in 0.50 M H_2SO_4 solution. Scan rate 2 mV s^{-1}

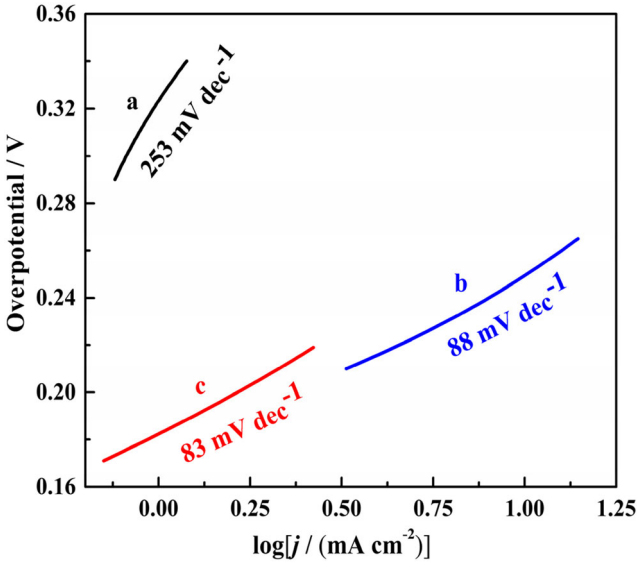

Fig. 6 Tafel plots of MWCNTs/GCE (**a**), CoS_2/GCE (**b**), and CoS_2/MWCNTs/GCE (**c**) in 0.50 M H_2SO_4 solution. Scan rate 1 mV s^{-1}

current density reached 29 mA cm^{-2}, the required potential of CoS_2/MWCNTs/GCE (− 303 mV) shifted positively about 100 mV compared with that of pure CoS_2/GCE (− 401 mV). In addition, it was obvious that the current density of CoS_2/MWCNTs/GCE (73 mA cm^{-2}) was higher than that of CoS_2/GCE (29 mA cm^{-2}) and MWCNTs/GCE (3 mA cm^{-2}) at the potential of − 400 mV, indicating better conductivity of CoS_2/MWCNTs/GCE. The favorable electrocatalytic performances of CoS_2/MWCNTs/GCE were attributed to the introduction of MWCNTs, which significantly alleviated the aggregation of CoS_2 and increased the effective surface area, thus facilitated the diffusion of electrolytes and electrons to the electroactive electrocatalysts, leading to more exposed catalytic active sites of CoS_2 and increased electronic conductivity.

To gain further insights into the HER kinetics, Tafel plots of as-prepared electrodes were investigated (Fig. 6). The linear regions of Tafel plots fitted the Tafel equation as follows.

$$\eta = a + \mathrm{b}\log j \tag{2}$$

where a was the constant, b the Tafel slope (mV dec^{-1}), and j the current density (mA cm^{-2}). The CoS_2/GCE and MWCNTs/GCE exhibited Tafel slopes of 88 and 253 mV dec^{-1}, respectively, while the slope of CoS_2/MWCNTs/GCE was 83 mV dec^{-1}, demonstrating faster HER kinetics of CoS_2/MWCNTs/GCE.

To gain a direct comparison, electrocatalytic performances toward HER of CoS_2-based electrodes reported in literatures are listed in Table 1. It was clearly observed that the electrocatalytic activity of CTAB-assisted synthesized CoS_2/MWCNT-based electrode in this work was higher or comparable with those in reported literatures, showing that as-prepared CoS_2/MWCNT-based electrode exhibited excellent electrocatalytic performances.

EIS measurement was carried out to obtain kinetic parameters of HER at the electrode/electrolyte interface with AC perturbation of 5 mV in the frequency range from 10^5 to 10^{-2} Hz. Shown in Fig. 7 were Nyquist plots of as-prepared modified electrodes, and the insert was an equivalent circuit for fitting the impedance data of CoS_2/MWCNTs/GCE, where R_s was the resistance at electrode/electrolyte interface, R_{ct} the charge transfer resistance, Z_w the Warburg resistance, and *CPE* the constant phase element.

It was obviously observed that all the Nyquist plots consisted of two regions: a semicircle at high frequencies and a linear part at low frequencies. R_{ct} for MWCNTs/GCE, CoS_2/GCE, and CoS_2/MWCNTs/GCE were 154, 700, and 300 Ω, respectively, indicating faster HER kinetics of CoS_2/MWCNTs/GCE than that of CoS_2/GCE. The lower R_{ct} of CoS_2/MWCNTs/GCE originated from the excellent conductivity of MWCNTs.

Table 1 Comparison of HER electrocatalytic performance of CoS_2-based electrodes

Electrode materials	Electrolytes	Tafel slope (mV dec^{-1})	η_{10}[a] (mV)	Ref.
CoS_2	0.50 M H_2SO_4	88	538	[44]
CoS_2/Ti	1.0 M KOH	133	244	[45]
CoS_2/RGO[b]	0.50 M H_2SO_4	327	300	[46]
CNF[c]@CoS_2	1.0 M KOH	66.8	110	[47]
CoS_2/CNTs	0.50 M H_2SO_4	114	160	[48]
MoS_2/CoS_2/CC[d]	0.50 M H_2SO_4	73.4	87	[49]
CoS_2/RGO	0.50 M H_2SO_4	285	143	[50]
CoS_2/MWCNTs	0.50 M H_2SO_4	83	257	This work

[a] Overpotential at cathodic current density of 10 mA cm^{-2}

[b] Reduced graphene oxide

[c] Carbon nanofiber

[d] Carbon cloth

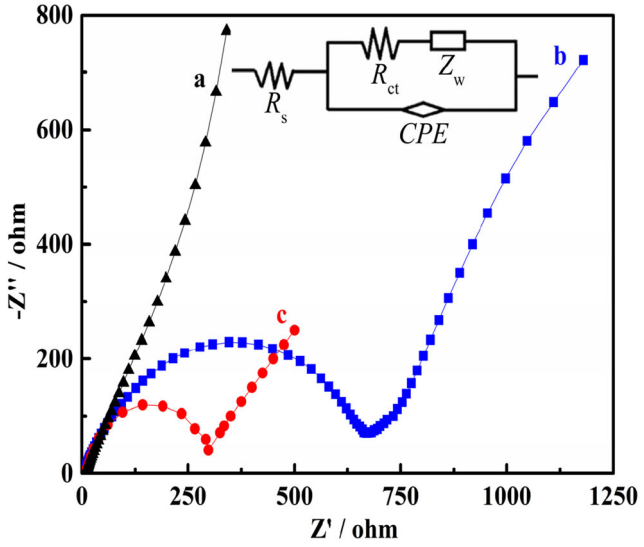

Fig. 7 Nyquist plots of MWCNTs/GCE (**a**), CoS_2/GCE (**b**), and CoS_2/MWCNTs/GCE (**c**) in 0.50 M H_2SO_4 solution

Besides the electrocatalytic activity, stability was another significant criterion to evaluate an advanced electrocatalyst. To investigate the long-term cycling stability of as-prepared CoS_2/MWCNTs/GCE in acidic environment, polarization curves were recorded after performing continuous cyclic voltammetry scans between − 0.6 and + 0.1 V at 50 mV s^{-1} for 1000 cycles and shown in Fig. 8. No obvious differences on onset potential or current density were observed between the initial plot and the last one, indicating that the CoS_2/MWCNTs/GCE exhibited excellent long-term stability for HER.

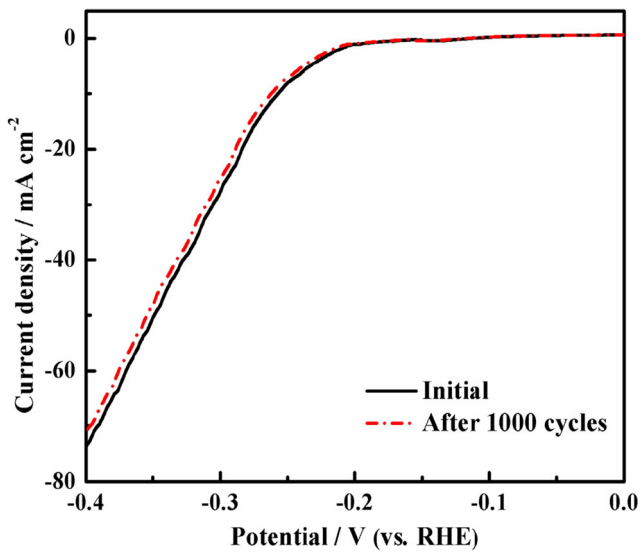

Fig. 8 Polarization curves of CoS_2/MWCNTs/GCE before and after 1000 CV scans in 0.50 M H_2SO_4 solution. Scan rate 2 mV s^{-1}

Conclusion

In this work, a novel CoS_2/MWCNT nanocomposite for HER was designed and constructed hydrothermally in the presence of CTAB. Compared with CoS_2/GCE and MWCNTs/GCE, CoS_2/MWCNTs/GCE required much lower potential (− 257 mV) to reach the current density of 10 mA cm^{-2}. Meanwhile, CoS_2/MWCNTs/GCE exhibited low Tafel slope (83 mV dec^{-1}), low charge transfer resistance (300 Ω), and long-term stability. The outstanding electrocatalytic activity of as-prepared CoS_2/MWCNT nanocomposite was attributed to the highly exposed sulfur edges of CoS_2 and excellent electrical conductivity of MWCNTs. CoS_2/MWCNT nanocomposite was a promising candidate for highly efficient electrocatalyst for practical hydrogen evolution through water splitting under acidic conditions.

Acknowledgements This work was supported by the Longshan Academic Talent Research Supporting Program of SWUST (17LZX406), the National Basic Research Program of China (2014CB846003), and the National Science and Technology Supported Program (2014BAC13B05). Also, we are grateful for the help of Analytical and Testing Center of Southwest University of Science and Technology.

References

1. Fetohi AE, Hameed RMA, El-Khatib KM, Souaya ER (2012) Ni–P and Ni–Co–P coated aluminum alloy 5251 substrates as metallic bipolar plates for PEM fuel cell applications. Int J Hydrog Energy 37(9):7677–7688
2. Zhang G, Liu HJ, Qu JH, Li JH (2016) Two-dimensional layered MoS_2: rational design, properties and electrochemical applications. Energy Environ Sci 9(4):1190–1209
3. Cobo S, Heidkamp J, Jacques PA, Fize J, Fourmond V, Guetaz L, Jousselme B, Ivanova V, Dau H, Palacin S (2012) A janus cobalt-based catalytic material for electro-splitting of water. Nat Mater 11(9):802–807
4. He P, Yi XF, Ma YJ, Wang W, Dong FQ, Du LC, Liu HT (2010) Effect of Gd_2O_3 on the hydrogen evolution property of nickel–cobalt coatings electrodeposited on titanium substrate. J Phys Chem Solids 72(11):1261–1264
5. Zou XX, Zhang Y (2015) Noble metal-free hydrogen evolution catalysts for water splitting. Chem Soc Rev 44(15):5148–5180
6. Walter MG, Warren EL, McKone JR, Boettcher SW, Mi Q, Santori EA, Lewis NS (2010) Solar water splitting cells. Chem Rev 110(11):6446–6473
7. Ding SS, He P, Feng WR, Li L, Zhang GL, Chen JC, Dong FQ, He HC (2016) Novel molybdenum disulfide nanosheets–decorated polyaniline: preparation, characterization and enhanced electrocatalytic activity for hydrogen evolution reaction. J Phys Chem Solids 91:41–47
8. Chen Z, Cummins D, Reinecke BN, Clark E, Sunkara MK, Jaramillo TF (2011) Core-shell MoO_3-MoS_2 nanowires for hydrogen evolution: a functional design for electrocatalytic materials. Nano Lett 11(10):4168–4175
9. Gong Z, Wang GC, Yang L, Liu HJ, Qu JH, Li JH (2016) Highly active and stable catalysts of phytic acid-derivative transition metal

phosphides for full water splitting. J Am Chem Soc 138(44): 14686–14693
10. Liu TT, Ma X, Liu DN, Hao S, Du G, Ma YJ, Asiri AM, Sun XP, Chen L (2017) Mn-Co-P nanosheets array: an efficient electrocatalyst for hydrogen evolution reaction with enhanced activity at all pH values. ACS Catal 7(1):98–102
11. Qu Y, Medina H, Wang SW, Wang YC, Chen CW, Su TY, Manikandan A, Wang K, Shih YC, Chang JW (2016) Wafer scale phase-engineered 1T- and 2H-$MoSe_2$/Mo core-shell 3D-hierarchical nanostructures toward efficient electrocatalytic hydrogen evolution reaction. Adv Mater 28(44):9831–9838
12. Kayan DB, İlhan M, Koçak D (2017) Chitosan-based hybrid nanocomposite on aluminium for hydrogen production from water. Ionics 4:1–7
13. Li W, Gao X, Wang X, Xiong D, Huang PP, Song WG, Bao X, Liu L (2016) From water reduction to oxidation: janus Co-Ni-P nanowires as high-efficiency and ultrastable electrocatalysts for over 3000h water splitting. J Power Sources 330:156–166
14. Li TH, Chen CJ, Lu YR, Dong CL, Liu RS (2016) Synergistic-effect-controlled $CoTe_2$/carbon nanotube hybrid material for efficient water oxidation. J Phys Chem C 120(49):28093–28099
15. Wang SQ, Xia WY, Liang ZS, Liu ZL, Xu CW, Li QY (2017) NiO/C enhanced by noble metal (Pt, Pd, Au) as high-efficient electrocatalyst for oxygen evolution reaction in water oxidation to obtain high purity hydrogen. Ionics 23:2161–2166
16. Crețu R, Kellenberger A, Vaszilcsin N (2013) Enhancement of hydrogen evolution reaction onplatinum cathode by proton carriers. Int J Hydrog Energy 38(27):11685–11694
17. Li KD, Zhang JF, Wu R, Yu YF, Zhang B (2016) Anchoring CoO domains on $CoSe_2$ nanobelts as bifunctional electrocatalysts for overall water splitting in neutral media. Adv Sci 3(6):1500426
18. Faber MS, Jin S (2014) Earth-abundant inorganic electrocatalysts and their nanostructures for energy conversion applications. Energy Environ Sci 7(11):3519–3542
19. Zhu YB, Liu T, Li LM, Song SL, Ding R (2018) Nickel-based electrodes as catalysts for hydrogen evolution reaction in alkaline media. Ionics: 24. https://doi.org/10.1007/s11581-017-2270-z
20. Wu C, Yang YJ, Dong D, Zhang YH, Li JH (2017) In situ coupling of CoP polyhedrons and carbon nanotubes as highly efficient hydrogen evolution reaction electrocatalyst. Small 13(15):1602873
21. Huang Y, Gong QF, Song XN, Feng K, Nie KQ, Zhao FP, Wang YY, Zeng M, Zhong J, Li YG (2016) Mo_2C nanoparticles dispersed on hierarchical carbon microflowers for efficient electrocatalytic hydrogen evolution. ACS Nano 10(12):11337–11343
22. Morales-Guio CG, Stern LA, Hu XL (2014) Nanostructured hydrotreating catalysts for electrochemical hydrogen evolution. Chem Soc Rev 43(18):6555–6569
23. Huang ZP, Wang CF, Pan L, Tian F, Zhang XX, Zhang C (2013) Enhanced photoelectrochemical hydrogen production using silicon nanowires@MoS_3. Nano Energy 2(6):1337–1346
24. Gupta S, Patel N, Fernandes R, Kadrekar R, Dashora A, Yadav AK, Bhattacharyya D, Jha SN, Miotello A, Kothari DC (2016) Co–Ni–B nanocatalyst for efficient hydrogen evolution reaction in wide pH range. Appl Catal B Environ 192:126–133
25. Ashassi-Sorkhabi H, Rezaei-Moghadam B, Asghari E, Bagheri R, Hosseinpour Z (2017) Fabrication of bridge like Pt@MWCNTs/CoS_2 electrocatalyst on conductive polymer matrix for electrochemical hydrogen evolution. Chem Eng J 308:275–288
26. Wu C, Zhang YH, Dong D, Xie HM, Li JH (2017) Co_9S_8 nanoparticles anchored on nitrogen and sulfur dual-doped carbon nanosheets as highly efficient bifunctional electrocatalyst for oxygen evolution and reduction reactions. Nano 9(34):12432–12440
27. Cui Y, Zhou CW, Li XZ, Gao Y, Zhang J (2017) High performance electrocatalysis for hydrogen evolution reaction using nickel-doped CoS_2 nanostructures: experimental and DFT insights. Electrochim Acta 228:428–435
28. Ouyang CB, Wang X, Wang SY (2015) Phosphorus-doped CoS_2 nanosheet arrays as ultra-efficient electrocatalysts for the hydrogen evolution reaction. Chem Commun 51(75):14160–14163
29. Fang L, Zhang Y, Guan YX, Zhang HJ, Wang SL, Wang Y (2017) Specific synthesis of CoS_2 nanoparticles embedded in porous Al_2O_3 nanosheets for efficient hydrogen evolution and enhanced lithium storage. J Mater Chem A 5(6):2861–2869
30. Faber MS, Lukowski MA, Ding Q, Kaiser NS, Jin S (2014) Earth-abundant metal pyrites (FeS_2, CoS_2, NiS_2 and their alloys) for highly efficient hydrogen evolution and polysulfide reduction electrocatalysis. J Phys Chem C 118(37):21347–21356
31. Lu XB, Wen ZH, Li JH (2006) Hydroxyl-containing antimony oxide bromide nanorods combined with chitosan for biosensors. Biomaterials 27(33):5740–5747
32. Li YG, Wang HL, Xie LM, Liang YY, Hong GS, Dai HJ (2011) MoS_2 nanoparticles grown on graphene: an advanced catalyst for the hydrogen evolution reaction. J Am Chem Soc 133(19):7296–7299
33. Lin TW, Liu CJ, Lin JY (2013) Facile synthesis of MoS_3/carbon nanotube nanocomposite with high catalytic activity toward hydrogen evolution reaction. Appl Catal B Environ 134-135(17):75–82
34. Pal S, Sahoo M, Veettil VT, Tadi KK, Ghosh A, Satyam P, Biroju RK, Ajayan PM, Nayak SK, Narayanan TN (2017) Covalently connected carbon nanotubes as electrocatalysts for hydrogen evolution reaction through band engineering. ACS Catal 7:2676–2684
35. Zhang YJ, Yi W, Yang L, Li D, Li JH (2004) Functionalization of single-walled carbon nanotubes with Prussian blue. Electrochem Commun 6(11):1180–1184
36. Lin TW, Liu CJ, Dai CS (2014) Ni_3S_2/carbon nanotube nanocomposite as electrode material for hydrogen evolution reaction in alkaline electrolyte and enzyme-free glucose detection. Appl Catal B Environ 154-155(7):213–220
37. Lota G, Fic K, Frackowiak E (2011) Carbon nanotubes and their composites in electrochemical applications. Energy Environ Sci 4(5):1592–1605
38. Chakoli AN, Wan J, Feng JT, Amirian M, Sui JH, Cai W (2009) Functionalization of multiwalled carbon nanotubes for reinforcing of poly(l-lactide-co-ε-caprolactone) biodegradable copolymers. Appl Surf Sci 256(1):170–177
39. Xing JC, Zhu YL, Li MY, Jiao QJ (2014) Hierarchical mesoporous CoS_2 microspheres: morphology-controlled synthesis and their superior pseudocapacitive properties. Electrochim Acta 149:285–292
40. Li T, Zhang CZ, Fan X, Li Y, Song M (2017) Degradation of oxidized multi-walled carbon nanotubes in water via photo-Fenton method and its degradation mechanism. Chem Eng J 323: 37–46
41. Tang JH, Shen JF, Li N, Ye MX (2014) A free template strategy for the synthesis of CoS_2-reduced graphene oxide nanocomposite with enhanced electrode performance for supercapacitors. Ceram Int 40(10):15411–15419
42. Nouralishahi A, Khodadadi AA, Mortazavi Y, Rashidi A, Choolaei M (2014) Enhanced methanol electro-oxidation activity of Pt/MWCNTs electro-catalyst using manganese oxide deposited on MWCNTs. Electrochim Acta 147:192–200
43. Mitra A, Mahapatra AS, Mallick A, Chakrabarti PK (2017) Enhanced microwave absorption and magnetic phase transitions of nanoparticles of multiferroic $LaFeO_3$ incorporated in multiwalled carbon nanotubes (MWCNTs). J Magn Magn Mater 435:117–125
44. Chen LL, Yang WX, Liu XJ, Jia JB (2017) Flower-like CoS_2/MoS_2 nanocomposite with enhanced electrocatalytic activity for hydrogen evolution reaction. Int J Hydrog Energy 42(17):12246–12253
45. Zhang HC, Li YJ, Zhang GX, Wan PB, Xu TH, Wu XC, Sun XM (2014) Highly crystallized cubic cattierite CoS_2 for electrochemically hydrogen evolution over wide pH range from 0 to 14. Electrochim Acta 148:170–174

46. Su C, Xiang JY, Wen FS, Song LZ, Mu CP, Xu DY, Hao CX, Liu ZY (2016) Microwave synthesized three-dimensional hierarchical nanostructure CoS_2/MoS_2 growth on carbon fiber cloth: a bifunctional electrode for hydrogen evolution reaction and supercapacitor. Electrochim Acta 212:941–949
47. Gu HH, Huang YP, Zuo LZ, Fan W, Liu TX (2016) Electrospun carbon nanofiber@CoS_2 core/sheath hybrid as efficient all-pH hydrogen evolution electrocatalyst. Inorg Chem Front 3(10):1280–1288
48. Liu YR, Hu WH, Li X, Dong B, Shang X, Han GQ, Chai YM, Liu YQ, Liu CG (2016) Facile one-pot synthesis of CoS_2-MoS_2/CNTs as efficient electrocatalyst for hydrogen evolution reaction. Appl Surf Sci 384:51–57
49. Huang JL, Hou DM, Zhou YC, Zhou WJ, Li GQ, Tang ZH, Li LG, Chen SW (2015) MoS_2 nanosheet-coated CoS_2 nanowire arrays on carbon cloth as three-dimensional electrodes for efficient electrocatalytic hydrogen evolution. J Mater Chem A 3(45):22886–22891
50. Xing W, Zhang Y, Xue QZ, Yan ZF (2015) Highly active catalyst of two-dimensional CoS_2/graphene nanocomposites for hydrogen evolution reaction. Nanoscale Res Lett 10(1):488–494